attenuates pressure-overload-induced cardiac hypertrophy. *J Cell Biochem.* 2007;100:1086–1099.
20. Liao Y, Asakura M, Takashima S, Ogai A, Asano Y, Shintani Y, Minamino T, Asanuma H, Sanada S, Kim J, Kitamura S, Tomoike H, Hori M, Kitakaze M. Celiprolol, a vasodilatory beta-blocker, inhibits pressure overload-induced cardiac hypertrophy and prevents the transition to heart failure via nitric oxide-dependent mechanisms in mice. *Circulation.* 2004;110:692–699.
21. Elsner D, Riegger GA. Characteristics and clinical relevance of animal models of heart failure. *Curr Opin Cardiol.* 1995;10:253–259.
22. Lee WL, Chen JW, Ting CT, Ishiwata T, Lin SJ, Korc M, Wang PH. Insulin-like growth factor I improves cardiovascular function and suppresses apoptosis of cardiomyocytes in dilated cardiomyopathy. *Endocrinology.* 1999;140:4831–4840.
23. An D, Kewalramani G, Chan JK, Qi D, Ghosh S, Pulinilkunnil T, Abrahani A, Innis SM, Rodrigues B. Metformin influences cardiomyocyte cell death by pathways that are dependent and independent of caspase-3. *Diabetologia.* 2006;49:2174–2184.
24. Terai K, Hiramoto Y, Masaki M, Sugiyama S, Kuroda T, Hori M, Kawase I, Hirota H. AMP-activated protein kinase protects cardiomyocytes against hypoxic injury through attenuation of endoplasmic reticulum stress. *Mol Cell Biol.* 2005;25:9554–9575.
25. Mangano DT. Effects of acadesine on myocardial infarction, stroke, and death following surgery: a meta-analysis of the 5 international randomized trials: the Multicenter Study of Perioperative Ischemia (McSPI) Research Group. *JAMA.* 1997;277:325–332.
26. Kitakaze M, Takashima S, Minamino T, Node K, Shinozaki Y, Mori H, Kuzuya T, Hori M. Improvement by 5-amino-4-imidazole carboxamide riboside of the contractile dysfunction that follows brief periods of ischemia through increases in ecto-5-nucleotidase activity and adenosine release in canine hearts. *Jpn Circ J.* 1999;63:542–553.
27. Recchia FA, McConnell PI, Bernstein RD, Vogel TR, Xu X, Hintze TH. Reduced nitric oxide production and altered myocardial metabolism during the decompensation of pacing-induced heart failure in the conscious dog. *Circ Res.* 1998;83:969–979.
28. Chen ZP, Mitchelhill KI, Michell BJ, Stapleton D, Rodriguez-Crespo I, Witters LA, Power DA, Ortiz de Montellano PR, Kemp BE. AMP-activated protein kinase phosphorylation of endothelial NO synthase. *FEBS Lett.* 1999;443:285–289.
29. Zhang Y, Lee TS, Kolb EM, Sun K, Lu X, Sladek FM, Kassab GS, Garland T Jr, Shyy JY. AMP-activated protein kinase is involved in endothelial NO synthase activation in response to shear stress. *Arterioscler Thromb Vasc Biol.* 2006;26:1281–1287.
30. Davis BJ, Xie Z, Viollet B, Zou MH. Activation of the AMP-activated kinase by antidiabetes drug metformin stimulates nitric oxide synthesis in vivo by promoting the association of heat shock protein 90 and endothelial nitric oxide synthase. *Diabetes.* 2006;55:496–505.
31. Sun W, Lee TS, Zhu M, Gu C, Wang Y, Zhu Y, Shyy JY. Statins activate AMP-activated protein kinase in vitro and in vivo. *Circulation.* 2006; 114:2655–2662.
32. Swan JW, Anker SD, Walton C, Godsland IF, Clark AL, Leyva F, Stevenson JC, Coats AJ. Insulin resistance in chronic heart failure: relation to severity and etiology of heart failure. *J Am Coll Cardiol.* 1997;30:527–532.
33. Nielson C, Lange T. Blood glucose and heart failure in nondiabetic patients. *Diabetes Care.* 2005;28:607–611.
34. Fischer Y, Thomas J, Rosen P, Kammermeier H. Action of metformin on glucose transport and glucose transporter GLUT1 and GLUT4 in heart muscle cells from healthy and diabetic rats. *Endocrinology.* 1995;136: 412–420.
35. Russell RR 3rd, Bergeron R, Shulman GI, Young LH. Translocation of myocardial GLUT-4 and increased glucose uptake through activation of AMPK by AICAR. *Am J Physiol.* 1999;277:H643–H649.
36. Davila-Roman VG, Vedala G, Herrero P, de las Fuentes L, Rogers JG, Kelly DP, Gropler RJ. Altered myocardial fatty acid and glucose metabolism in idiopathic dilated cardiomyopathy. *J Am Coll Cardiol.* 2002;40: 271–277.
37. Sack MN, Rader TA, Park S, Bastin J, McCune SA, Kelly DP. Fatty acid oxidation enzyme gene expression is downregulated in the failing heart. *Circulation.* 1996;94:2837–2842.
38. Osorio JC, Stanley WC, Linke A, Castellari M, Diep QN, Panchal AR, Hintze TH, Lopaschuk GD, Recchia FA. Impaired myocardial fatty acid oxidation and reduced protein expression of retinoid X receptor-alpha in pacing-induced heart failure. *Circulation.* 2002;106:606–612.
39. Paolisso G, Gambardella A, Galzerano D, D'Amore A, Rubino P, Verza M, Teasuro P, Varricchio M, D'Onofrio F. Total-body and myocardial substrate oxidation in congestive heart failure. *Metabolism.* 1994;43: 174–179.
40. Horman S, Beauloye C, Vertommen D, Vanoverschelde JL, Hue L, Rider MH. Myocardial ischemia and increased heart work modulate the phosphorylation state of eukaryotic elongation factor-2. *J Biol Chem.* 2003; 278:41970–41976.
41. Inoki K, Zhu T, Guan KL. TSC2 mediates cellular energy response to control cell growth and survival. *Cell.* 2003;115:577–590.
42. Shinbane JS, Wood MA, Jensen DN, Ellenbogen KA, Fitzpatrick AP, Scheinman MM. Tachycardia-induced cardiomyopathy: a review of animal models and clinical studies. *J Am Coll Cardiol.* 1997;29: 709–715.
43. Montagnani M, Chen H, Barr VA, Quon MJ. Insulin-stimulated activation of eNOS is independent of Ca^{2+} but requires phosphorylation by Akt at Ser(1179). *J Biol Chem.* 2001;276:30392–30398.
44. Fulton D, Gratton JP, McCabe TJ, Fontana J, Fujio Y, Walsh K, Franke TF, Papapetropoulos A, Sessa WC. Regulation of endothelium-derived nitric oxide production by the protein kinase Akt. *Nature.* 1999;399: 597–601.
45. Shiojima I, Walsh K. Regulation of cardiac growth and coronary angiogenesis by the Akt/PKB signaling pathway. *Genes Dev.* 2006;20: 3347–3365.

CLINICAL PERSPECTIVE

Metformin is widely used as an antidiabetic drug with an insulin-sensitizing effect. A large-scale clinical trial (the UK Prospective Diabetes Study [UKPDS] 34) has shown that metformin therapy decreased the risk of cardiovascular death and the incidence of myocardial infarction associated with diabetes mellitus; metformin reduced the hemoglobin A_{1c} levels in treated patients to the same extent as in the other patients treated with conventional therapies. These results suggest that metformin might exert cardioprotective effects beyond its glucose-lowering action such as either activation of AMP-activated protein kinase (AMPK) or elevation of nitric oxide. Metformin is known to activate AMPK, which mediates potent cardioprotection against ischemia/reperfusion injury. AMPK also is activated in experimental failing myocardium, suggesting that activation of AMPK is beneficial for the pathophysiology of heart failure. The present study demonstrated that long-term oral administration of metformin prevents the progression of heart failure as indicated by hemodynamic and echocardiographic parameters. Metformin also promoted phosphorylation of both AMPK and endothelial nitric oxide synthase, increased plasma nitric oxide levels, and improved insulin resistance. As a result of these effects, metformin decreased apoptosis and improved cardiac function in failing canine hearts. Interestingly, another AMPK activator (AICAR) had effects equivalent to those of metformin, suggesting the primary role of AMPK activation in reducing apoptosis and preventing heart failure. Drugs that activate AMPK, especially metformin, may provide a novel strategy for the treatment of heart failure in clinical settings.

Supplemental Methods

The animal experiments were approved by the National Cardiovascular Center Research Committee and were performed according to institutional guidelines.

Experimental Protocols

1) Effects of Metformin on Cardiomyocyte Viability and Apoptosis After Exposure to H_2O_2

To investigate whether metformin has a cardioprotective effect against damage due to H_2O_2 in vitro, we assessed cell viability and apoptosis in cultured cardiomyocytes using the 3-(4,5-dimethylthiazol-2-yl)-2,5-diphenyl tetrazolium bromide (MTT) assay and both the terminal deoxynucleotidyl transferase-mediated dUTP nick-end labeling (TUNEL) staining plus flow cytometry, respectively. The cells were cultured in serum-free media for 24 hours and then incubated in the presence of 50 μmol/L H_2O_2 for 24 hours. Cardiomyocytes were pretreated with either metformin (1 to 100 μmol/L) or 5-amino-4-imidazole-1-β-D-carboxamide ribofuranoside (AICAR; an AMPK activator) (500 μmol/L) for 60 minutes before the addition of H_2O_2. Other cells were preincubated with an AMPK inhibitor, compound-C (20 μmol/L) for 6 hours before the addition of either metformin or AICAR. Then cell viability and apoptosis were analyzed.

2) Effects of Metformin on Cardiac Performance in Dogs With Pacing-Induced Heart Failure

After pacemaker implantation, the dogs were randomly assigned to 3 groups as follows: 1) a group that received a normal diet and drinking water (Pacing group, n=8), 2) a group that received metformin orally at a dose of 100 mg/kg/day (Pacing+Met group, n=8), and 3) a group received AICAR

subcutaneously every other day at 5 mg/kg (Pacing+AICAR group, n=4). We also performed a sham operation in another 6 dogs (Sham group, n=6). The dose of metformin (100 mg/kg/day) was selected because our preliminary study showed that this was the maximum dose that did not induce hypoglycemia (data not shown). The dose of AICAR (5 mg/kg subcutaneously on alternate days) was selected because we preliminarily confirmed that phosphorylation of AMPK was elevated at least 48 hours after subcutaneous injection of AICAR, by reference to previous report in rats, due to the lack of any data for dogs (Supplemental Figures).[1] Echocardiography was performed and hemodynamic parameters were measured before and after 4 weeks of right ventricular (RV) pacing. After assessment of these parameters, each heart was excised and divided into three parts for immunoblotting, quantitative reverse-transcriptase polymerase chain reaction (PCR), and histological examination.

Materials

1, 1-Dimethylbiguanide hydrochloride (metformin hydrochloride) was a kind gift from Nippon Shinyaku Co. Ltd. (Kyoto, Japan), while AICAR (an AMPK activator) and compound-C (an AMPK inhibitor) were purchased from Calbiochem (California, USA). Antibodies directed against endothelial nitric oxide synthase (eNOS) were obtained from Affinity BioReagents (Colorado, USA). Other antibodies were purchased from Cell Signaling Technology (Massachusetts, USA).

Cell Culture

Primary cultures of cardiomyocytes were prepared from ventricles of 1-day-old Wistar rats, as described previously.[2] In brief, cardiomyocytes were plated at a density of 5×10^5 cells/mL on

collagen-coated culture dishes and incubated in standard medium (DMEM with 10% FBS) for 72 hours, after which incubation was continued under serum-free conditions for 48 hours.

Cell Viability Assay (MTT Assay)

Cell viability was analyzed by a nonradioactive cell proliferation assay using MTT, as described previously with minor modifications[3].

Assessment of Cardiomyocyte Apoptosis

To investigate the influence of metformin on cardiomyocyte viability, TUNEL assay was performed as reported previously.[3] Apoptosis was also quantified by flow cytometry (FACScan; Becton, Dickinson and Company, New Jersey, USA) after cells were stained with annexin V and propidine iodide (PI) according to the manufacturer's instructions (Annexin V-FITC Apoptosis Detection Kit; Sigma, Saint Louis, USA).

Canine Pacing Model

Beagle dogs (Oriental Yeast Co. Ltd, Tokyo, Japan) weighing 8 to 10 kg were sedated with intravenous sodium pentobarbital at a dose of 25 mg/kg. After intubation with a cuffed endotracheal tube, anesthesia was maintained with 0.5 % to 1% isoflurane and an equal mixture of air and oxygen. Ventilation was provided with a tidal volume of 22 mL/kg at a rate of 15 times per minute. A bipolar pacing lead (Model BT-45P, Star Medical Inc., Tokyo, Japan) was advanced under fluoroscopic guidance through the right jugular vein to the RV apex and was connected to a programmable pacemaker (VOO mode; Model SIP-501, Star Medical Inc., Tokyo, Japan) that was implanted in a

subcutaneous pocket in the neck. The success of this procedure was confirmed by electrocardiography. Cefazolin sodium (1 g) was given intravenously after surgery, and the dogs were allowed to recover for a few hours. Then heart failure was induced by rapid RV pacing at a rate of 230 beats per minute for 4 weeks, as reported previously.[4]

Echocardiography

Transthoracic echocardiography was performed by using an echocardiographic system equipped with a 4-MHz phased-array transducer (SONOS 5500, PHILIPS, Eindhoven, the Netherlands) in conscious dogs before pacemaker implantation and 30 minutes after the cessation of right ventricular (RV) pacing at 4 weeks. A two-dimensional short-axis view of the left ventricle was obtained at the level of the papillary muscles. All measurements were made by two observers, who were blinded with respect to the source of the tracings.

Hemodynamic Studies

Both left ventricular end-diastolic pressure (LVEDP) and mean aortic pressure were measured by pressure transducers using a 5 Fr pig tail catheter (Terumo Co. Ltd., Tokyo, Japan) that was inserted into the left ventricle from the left femoral artery. The mean pulmonary artery pressure (PAP) and the pulmonary capillary wedge pressure (PCWP) were measured using a 7 Fr Swan-Ganz catheter (American Edwards Laboratories, California, USA). Cardiac output (CO) was determined at least three times by the thermodilution technique. Systemic vascular resistance (SVR) was calculated as follows: (mean aortic pressure-right atrial pressure) × 80/CO.

Histological examination

The collagen volume fraction was examined in sections of the left ventricular (LV) free wall, after excluding vessels, artifacts, minor scars, and incomplete tissue. Specimens were stained with Masson's trichrome stain to evaluate the extent of interstitial fibrosis, as described previously.[5] The area of stained tissue was calculated as a percentage of the total area within a field by using Scion image software (Beta 4.0.2).

Quantitative Reverse-Transcriptase PCR

The quantitative reverse-transcriptase PCR was performed as described previously.[6] Total RNA was extracted from LV myocardium with RNA-Bee-RNA Isolation Reagent (Tel-Test, Texas, USA). Then 1,000 ng of total RNA was reverse transcribed and amplified with an Omniscript RT Kit (Qiagen, Hilden, Germany) according to the manufacturer's protocol.

Oligonucleotide primers and TaqMan probes for canine atrial natriuretic peptide (ANP) (Cf 02705687_g1), canine transforming growth factor-β1 (TGF-β1) (Cf 02741608_m1), and canine ribosomal protein S18 (Cf 02681523_g1) were purchased from Applied Biosystems (California, USA). Both Taqman probe and primer designs were optimized to enhance stability on the basis of the known sequences of canine brain natriuretic peptide (BNP)[7] and canine endothelial NO synthase (eNOS).[8] We used the following probes, sense primers, and antisense primers: 5'-FAM-CAGTTGGCCCTGGAA-MGB-3', 5'-GAAGGACGCAGTTTCAGAGCTG -3' and 5'-AAAGCACCCTGACTTGTGCATC-3' for canine BNP; and

5'-FAM-CCTGGAGGATGTGGC-MGB-3', 5'-AACCTGTGTGACCCTCATCGAT-3' and 5'-TCACTTTGGCCAGCTGGTAACT-3' for canine eNOS, respectively.

Immunoblotting

Immunoblotting was performed as described previously.[9] A Bio-Rad ChemiDoc XRS system (Bio-Rad Laboratories, Inc., California, USA) was used for chemiluminescence imaging and immunoreactive bands were quantified with Bio-Rad Quantity One 1-D analysis software (Bio-Rad Laboratories, Inc., California, USA).

Measurement of Nitric Oxide End-Products

The plasma level of nitric oxide (NO) metabolic end-products (nitrite + nitrate) was measured by the Griess method, as reported previously.[10] Subsequently, ΔNO was defined as the difference between the plasma NO level before and after 4 weeks of RV pacing.

Metabolic Parameters

All dogs were fed a standard diet with a fixed carbohydrate and fat content (DS-A, Oriental Yeast Co. Ltd, Tokyo, Japan). After fasting for 14 hours, metabolic parameters such as the plasma levels of glucose, lactate, free fatty acids (FFA), and insulin were measured with a quick-auto-neo-GLU-HK (Shino-Test Corporation, Tokyo, Japan.), Determiner LA (KYOWA MEDEX Co., Ltd., Tokyo, Japan.), NEFA-SS Eiken, Eiken Chemical Co., Ltd., Tokyo, Japan.), and YK060 Insulin ELISA Kit (Yanaihara Institute Inc. Shizuoka, Japan), respectively. Insulin resistance was assessed from the fasting insulin and glucose levels by the homeostasis model assessment-insulin resistance (HOMA-IR) method, i.e.,

HOMA-IR is [fasting glucose (mmol/L) × fasting insulin (μU/mL)] / 22.5.[11] The levels of norepinephrine and angiotensin II were measured by using a CA test TOSOH (Tosoh Corporation, Tokyo, Japan.) and a NEX-105 (125I)-Tyr4-Angiotensin II test (PerkinElmer Inc., Massachusetts, USA.), respectively. Myocardial substrate extraction was calculated as described previously.[12]

Measurement of Body Fat and Activity in Dogs

To examine the effects of metformin on body fat and physical activity in this dog model of pacing-induced heart failure, we measured body fat with a dog body fat counter (IBF-D02, Kao Corporation, Tokyo, Japan) and evaluated physical activity by using a pedometer (SE-MG10, SATO KEIRYOUKI MFG. Co., Ltd., Tokyo, Japan) attached to each dog's collar.

Supplemental Figures

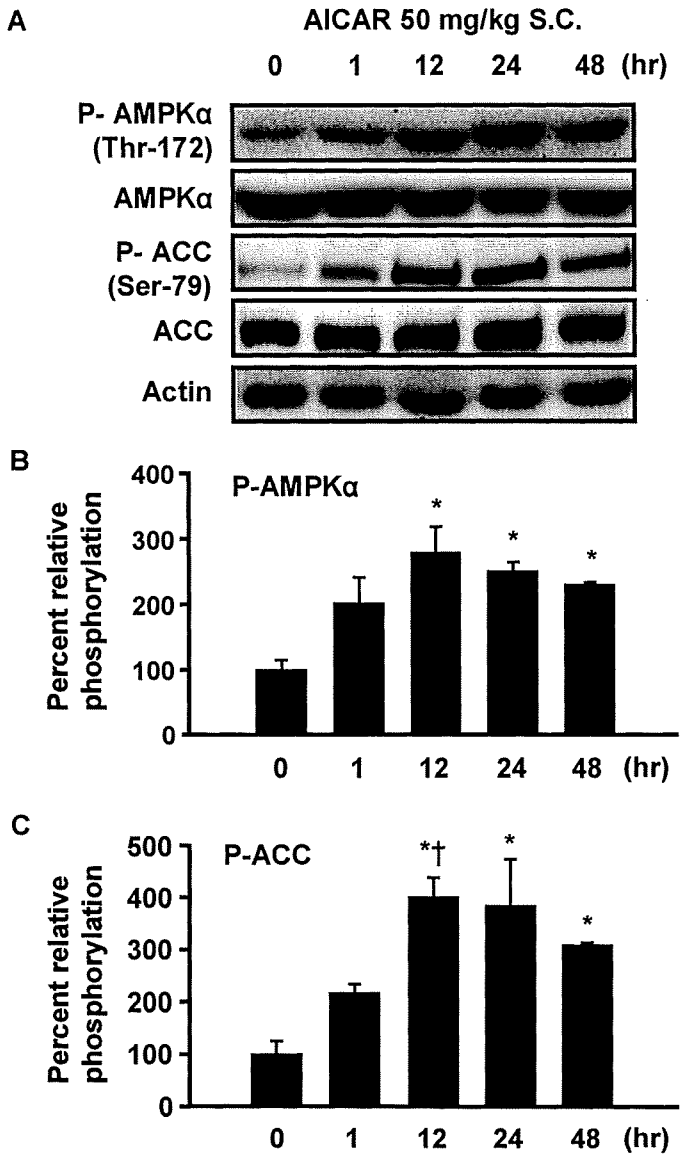

Changes in the phosphorylation of AMPKα and ACC in canine hearts after subcutaneous administration of AICAR. A) Representative immunoblots of phospho-AMPKα and ACC. **B)** and **C)** The percent relative phosphorylation of AMPKα and ACC, respectively. Values are the mean±SEM. *P<0.05 vs. no treatment; †P<0.05 vs. one hour after subcutaneous administration of AICAR. Representative results from 3 independent experiments are shown.

Supplemental References :

1. Li HL, Yin R, Chen D, Liu D, Wang D, Yang Q, Dong YG. Long-term activation of adenosine monophosphate-activated protein kinase attenuates pressure-overload-induced cardiac hypertrophy. *J Cell Biochem.* 2007;100:1086-1099.

2. Asakura M, Kitakaze M, Takashima S, Liao Y, Ishikura F, Yoshinaka T, Ohmoto H, Node K, Yoshino K, Ishiguro H, Asanuma H, Sanada S, Matsumura Y, Takeda H, Beppu S, Tada M, Hori M, Higashiyama S. Cardiac hypertrophy is inhibited by antagonism of ADAM12 processing of HB-EGF: metalloproteinase inhibitors as a new therapy. *Nat Med.* 2002;8:35-40.

3. Okada K, Minamino T, Tsukamoto Y, Liao Y, Tsukamoto O, Takashima S, Hirata A, Fujita M, Nagamachi Y, Nakatani T, Yutani C, Ozawa K, Ogawa S, Tomoike H, Hori M, Kitakaze M. Prolonged endoplasmic reticulum stress in hypertrophic and failing heart after aortic constriction: possible contribution of endoplasmic reticulum stress to cardiac myocyte apoptosis. *Circulation.* 2004;110:705-712.

4. Shinbane JS, Wood MA, Jensen DN, Ellenbogen KA, Fitzpatrick AP, Scheinman MM. Tachycardia-induced cardiomyopathy: a review of animal models and clinical studies. *J Am Coll Cardiol.* 1997;29:709-715.

5. Wakeno M, Minamino T, Seguchi O, Okazaki H, Tsukamoto O, Okada K, Hirata A, Fujita M, Asanuma H, Kim J, Komamura K, Takashima S, Mochizuki N, Kitakaze M. Long-term stimulation of adenosine A2b receptors begun after myocardial infarction prevents cardiac

remodeling in rats. *Circulation.* 2006;114:1923-1932.

6. Fujita M, Okuda H, Tsukamoto O, Asano Y, Hirata YL, Kim J, Miyatsuka T, Takashima S, Minamino T, Tomoike H, Kitakaze M. Blockade of angiotensin II receptors reduces the expression of receptors for advanced glycation end products in human endothelial cells. *Arterioscler Thromb Vasc Biol.* 2006;26:e138-142.

7. Lisy O, Redfield MM, Schirger JA, Burnett JC, Jr. Atrial BNP endocrine function during chronic unloading of the normal canine heart. *Am J Physiol Regul Integr Comp Physiol.* 2005;288:R158-162.

8. Fulton D, Papapetropoulos A, Zhang X, Catravas JD, Hintze TH, Sessa WC. Quantification of eNOS mRNA in the canine cardiac vasculature by competitive PCR. *Am J Physiol Heart Circ Physiol.* 2000;278:H658-665.

9. Tsukamoto O, Minamino T, Okada K, Shintani Y, Takashima S, Kato H, Liao Y, Okazaki H, Asai M, Hirata A, Fujita M, Asano Y, Yamazaki S, Asanuma H, Hori M, Kitakaze M. Depression of proteasome activities during the progression of cardiac dysfunction in pressure-overloaded heart of mice. *Biochem Biophys Res Commun.* 2006;340:1125-1133.

10. Asanuma H, Node K, Minamino T, Sanada S, Takashima S, Ueda Y, Sakata Y, Asakura M, Kim J, Ogita H, Tada M, Hori M, Kitakaze M. Celiprolol increases coronary blood flow and reduces severity of myocardial ischemia via nitric oxide release. *J Cardiovasc Pharmacol.* 2003;41:499-505.

11. Bonora E, Targher G, Alberiche M, Bonadonna RC, Saggiani F, Zenere MB, Monauni T, Muggeo M. Homeostasis model assessment closely mirrors the glucose clamp technique in the assessment of insulin sensitivity: studies in subjects with various degrees of glucose tolerance and insulin sensitivity. *Diabetes Care.* 2000;23:57-63.

12. Nikolaidis LA, Elahi D, Hentosz T, Doverspike A, Huerbin R, Zourelias L, Stolarski C, Shen YT, Shannon RP. Recombinant glucagon-like peptide-1 increases myocardial glucose uptake and improves left ventricular performance in conscious dogs with pacing-induced dilated cardiomyopathy. *Circulation.* 2004;110:955-961.

Biochemical and Biophysical Research Communications 385 (2009) 618–623

Contents lists available at ScienceDirect

Biochemical and Biophysical Research Communications

journal homepage: www.elsevier.com/locate/ybbrc

Extracellular protein kinase CK2 is a novel associating protein of Neuropilin-1

Yasunori Shintani [a,c,1], Seiji Takashima [a,b,*], Hisakazu Kato [a,b], Kazuo Komamura [c,2], Masafumi Kitakaze [d]

[a] Department of Cardiovascular Medicine, Osaka University Graduate School of Medicine, Suita, Osaka, Japan
[b] Department of Molecular Cardiology, Osaka University Graduate School of Medicine, Suita, Osaka, Japan
[c] Department of Cardiovascular Dynamics, Research Institute, National Cardiovascular Center, Osaka, Japan
[d] Cardiovascular Division of Medicine, National Cardiovascular Center, Suita, Japan

ARTICLE INFO

Article history:
Received 18 May 2009
Available online 30 May 2009

Keywords:
Neuropilin-1
Protein kinase CK2
VEGF
Semaphorin

ABSTRACT

Neuropilin-1 (NRP1) is a multifunctional transmembrane protein which has a short cytoplasmic region with no particular functional domain, and is considered to act as a co-receptor for both VEGFs and semaphorins. However, the molecular mechanisms by which NRP1 carries out such versatile functions are still poorly understood. Here we identified protein kinase CK2 holoenzyme as a novel NRP1 binding protein by our combined purification strategy using epitope-tag immunoprecipitation followed by reverse-phase column chromatography. Further we showed that CK2 binds to the extracellular domain of NRP1 which is also phosphorylated by CK2 both *in vitro* and *in vivo*. Our findings of novel molecular interactions and modification of NRP1 may provide a new clue to understand the diverse functions of NRP1.

Introduction

Neuropilin-1 (NRP1) was originally discovered as a co-receptor for semaphorin-3A (Sema3A), an axon repellent factor [1]. In addition, NRP1 also acts as a co-receptor for vascular endothelial growth factor (VEGF), a molecule with no sequence or structural homology to Sema3A [2]. Partly due to this interesting property of NRP1, a number of reports have been published and revealed that NRP1 is involved in a wide variety of both physiological and pathological processes; axon guidance [3], angiogenesis [4], tumor progression [5], metastasis [6], immunological maturation [7], and virus entry [8].

Recently it has been revealed that NRP1 functions are intriguingly versatile and vary among the cell types in which NRP1 is expressed [9–12]. Considering its short cytoplasmic region without a specific signalling domain, NRP1 is originally thought to function as a co-receptor working with plexins for semaphorins or with VEGFRs for VEGFs [13]. However the molecular mechanisms by which NRP1 produces such diverse effects are not fully explained by this deduction. This led us to hypothesize that additional molecular interactions between NRP1 and unknown molecules may exist. Therefore, the aim of this study was to uncover novel binding partners of NRP1 in order to understand the complex nature of NRP1 functions.

Materials and methods

Materials and primary cells. We utilized the following commercially available antibodies: anti NRP1 antibody (C-19, Santa Cruz), anti FLAG M2 (Sigma), anti CSNK2A1 (sc-6479, Santa Cruz) and anti CSNK2B (Calbiochem). Anti-Myc agarose was obtained from Clontech. Recombinant CK2 holoenzyme was purchased from KinaseDetect. CK2 inhibitor, DMAT (2-Dimethylamino-4, 5, 6, 7-tetrabromo-1H-benzimidazole) was obtained from Calbiochem. Both human umbilical vein endothelial cells (HUVEC) and human coronary artery smooth muscle cells (CASMC) were purchased from Clonetics. They were cultured in endothelial and smooth muscle cell medium (Clonetics) and used up to passage 5.

Expression vector and adenovirus constructs. Human NRP1 cDNA was obtained as described previously [2]. In this experiment, all constructions were performed using the Gateway system (Invitrogen) according to the manufacturer's instructions. With PCR primers, designed to include the stop codon of NRP1, the amplified fragment was inserted to pENTR/D-TOPO (Invitrogen), named pENTR/NRP1. To generate N-terminal-tagged NRP1, either the FLAG epitope (DYKDDDDK) or Myc epitope (EQKLISEEDL) was inserted just after signal sequence of NRP1 (between Lys^{26} and Cys^{27}) by PCR based mutagenesis using pENTR/NRP1 as a template. To identify the binding site on NRP1 for CK2A1, NRP1 lacking aa 54–274 (del A), NRP1 lacking aa 275–631 (del B), NRP1 lacking aa 632–823 (del C), or

* Corresponding author. Address: Department of Molecular Cardiology, Osaka University Graduate School of Medicine, 2-2 Yamadaoka, Suita, Osaka 565-0871, Japan. Fax: +816 8679 3473.
E-mail address: takasima@medone.med.osaka-u.ac.jp (S. Takashima).
[1] Present address: Translational Cardiovascular Therapeutics, William Harvey Research Institute, Queen Mary University of London, Charterhouse Square, London, EC1M 6BQ, UK.
[2] Present address: Faculty of Pharmaceutical Sciences, Department of Medical Pharmacy, Hyogo University of Health Sciences, Kobe, Japan.

0006-291X/$ - see front matter © 2009 Elsevier Inc. All rights reserved.
doi:10.1016/j.bbrc.2009.05.108

NRP1 lacking aa 876–923 (del cyto) was generated by PCR using either pENTR–FLAG–NRP1 or pENTR–Myc–NRP1 as a template. All NRP1 constructs were sequence-verified and recombined to the mammalian expression vector, pEF-DEST51 (Invitrogen). Adenovirus constructs were generated using the ViraPower Adenoviral Expression System (Invitrogen) essentially as described by the manufacturer. The supplied pAd/CMV/V5-DEST/lacZ was used as a control (Invitrogen).

Generation of stable cell lines. VEGFR2 cDNA was cloned into pENTR/D-TOPO from HUVEC cDNA. We generated Flp293 cells which stably expressed VEGFR2 using Flp-In system (Invitrogen) as previously described [9].

Identification of NRP1 binding proteins using metabolic labelling and high performance liquid chromatography (HPLC). After metabolic labelling with [^{35}S] methionine/cysteine for 8 h, a 100 mm dish of Flp293/VEGFR2 cells, in which 10 μg of Myc-NRP1 was transiently transfected 2 days beforehand, were lysed with lysis buffer (10 mM Tris–HCl pH 7.4, 150 mM NaCl, 1 mM EDTA, 0.5% NP40 and the protease inhibitor cocktail (Nakalai)) with or without phosphatase inhibitors (10 mM sodium fluoride, 1 mM orthovanadate), followed by immunoprecipitation with anti-Myc affinity gel for 1 h at 4 °C. A Myc-tagged unrelated gene (human FAM155B, NM_015686.2) was transfected in Flp293/VEGFR2 and used as a control. After extensive washing, bound proteins were boiled and eluted in sample buffer, followed by SDS–PAGE. The radioactivity was detected using a BAS imaging analyzer (Fuji). For further purification, the immunoprecipitates were eluted with elution buffer (0.3% trifluoroacetic acid (TFA), 0.1% octylglucoside and 5% acetonitrile). Then the eluate was applied to a phenyl reverse-phase HPLC column (4.6 × 250 mm, Nakalai). Fractions were eluted with a linear gradient of 0–80% acetonitrile at a flow rate of 0.5 ml/min. Each fraction was resolved by SDS–PAGE, and the radioactivity was detected by BAS. For identification, 6 × 100 mm dishes of Flp293/VEGFR2 cells transfected with Myc-NRP1 or FAM155B-Myc were immunoprecipitated with anti-Myc affinity gel, and followed by HPLC as same as above. The silver stained band was excised and analyzed by MALDI-TOF/MS (Hitachi High-Tech Manufacturing and Service Co., Ltd.).

Co-immunoprecipitation assay. Flp293/VEGFR2 cells were transfected with Myc-NRP1 or the Myc-tagged deletion mutants using Lipofectamine 2000. Two days after transfection the cells were lysed in lysis buffer (10 mM Tris–HCl, 150 mM NaCl, 1 mM EDTA, 0.5% NP40 and the protease inhibitor cocktail (Nakalai)). To confirm endogenous binding, HUVEC and CASMC in a 100 mm dish without forced expression were used. We then incubated with anti-NRP1 or control rabbit IgG with protein G Sepharose (GE healthcare) for 1 h at 4 °C. After extensive washing, immunoprecipitated samples were subjected to SDS–PAGE and immunoblotting. Metabolic labelling followed by immunoprecipitation for the deletion mutants of NRP1 was carried as described above.

In vitro kinase assay. HEK293T cells transfected with FLAG-tagged NRP1 were lysed with lysis buffer (10 mM Tris–HCl (pH 7.2), 300 mM NaCl, 1 mM $CaCl_2$, 1 mM $MnCl_2$, 1% NP40 and the protease inhibitor cocktail (Nakalai)), immunoprecipitated with ConA Sepharose (GE healthcare) for 2 h at 4 °C, followed by elution with 0.5 M mannopiranoside (Sigma). Further purification was performed using immunoprecipitation with FLAG agarose followed by FLAG peptide elution (100 μg/ml). The purified NRP1 was equilibrated in kinase buffer (20 mM MOPS (pH 7.0), 150 mM NaCl, 20 mM $MgCl_2$, 1 mM DTT, 20 μM cold ATP and 0.1% NP40), and then incubated with recombinant CK2 holoenzyme (100 ng) and 10 μCi of [γ-^{32}P] ATP (GE healthcare) at 30 °C for 30 min. The CK2 inhibitor, DMAT, was added at 1 μM in reaction buffer. Each sample was boiled in SDS sample buffer for 3 min, and eluted proteins were analyzed by SDS–PAGE. The gel was dried and subjected to autoradiography.

Phosphoamino acid analysis. Phosphoamino acid analysis was performed as described previously [14]. Briefly, purified NRP1 was incubated with CK2 holoenzyme in the presence of [γ-^{32}P] ATP as described above. The reaction mixture was then separated by SDS–PAGE, stained with Coomassie blue, and visualized by autoradiography. The radiolabelled band was excised from the gel and digested with trypsin. The digested sample was hydrolyzed by boiling in 6 M HCl for 60 min at 110 °C. The hydrolysate was lyophilized and resuspended in 5% TFA, 50% acetonitrile containing phosphoamino acid standards, and spotted onto thin-layer cellulose plates. Electrophoresis was performed using pH 1.9 buffer for the first dimension and pH 3.5 buffer (5% acetic acid, 0.5% pyridine) for the second dimension. The standards were then stained with ninhydrin, and the plates were analyzed by autoradiography.

In vivo kinase assay. HUVEC were transfected with either LacZ or FLAG-NRP1 adenovirus at MOI 25 in 60 mm dishes 2 days before assay. The medium was changed to phosphate-free DMEM (GIBCO) containing 2% dialysed FBS (GIBCO), labelled with ortho [^{32}P] orthophosphate (0.25 mCi/ml, GE healthcare) for 4–12 h. The CK2 inhibitor, DMAT, was added at 1 μM during the labelling period. The labelled cells were washed with sucrose buffer once, lysed with lysis buffer (10 mM Tris–HCl (pH 7.2), 150 mM NaCl, 10 mM sodium fluoride, 1% NP40 and the protease inhibitor cocktail (Nakalai)), and then immunoprecipitated with anti-FLAG agarose for 1 h at 4 °C. The eluted proteins were analyzed by SDS–PAGE. The gel was dried and subjected to autoradiography.

Results

Identification of protein kinase CK2 as a novel NRP1 binding protein

We have previously reported that NRP1 affects VEGFR2 expression before ligand binding and VEGFR2 degradation after forming the receptor complex via unknown mechanisms [9]. Therefore, we presume that NRP1 may have other associating molecules in the presence of VEGFR2.

Screening NRP1 immunoprecipitates from metabolically labelled Flp293/VEGFR2 cells transiently transfected with Myc-NRP1 yielded 3 candidate bands (Fig. 1A, lane 2). We chose Myc-tagged NRP1 because background signal was the lowest among tested epitope tags (data not shown). Interestingly the intensities of these bands decreased if phosphatase inhibitors were added in the lysis buffer (Fig. 1A, lane 4). These target proteins were further purified by reverse-phase HPLC, and the fraction analysis is shown in Fig. 1B. Among the 3 targets, we could clearly separate a 43 kDa NRP1-associated band in fraction 57 and a 25 kDa band in fraction 58. To identify these two bands, a large scale preparation without metabolic labelling was performed and both fractions visualized by silver stain. Although a large amount of immunoglobulin derived from the anti-Myc affinity gel masked the 25 kDa band in fraction 58, the 43 kDa NRP1-associated band was detected by silver stain (Fig. 1C). Peptide mass fingerprinting by MALDI-TOF/MS analysis of the digested 43 kDa band revealed that four peptides (QLYQTLTDYDIR, EAMEHPYFYTVVK, GGPNIITLADIVKDPVSR and EPFFHGHDNYDQLVR) matched to human protein kinase CK2 α subunit (CSNK2A1).

To confirm CSNK2A1 binding to NRP1, co-immunoprecipitation was carried out using Flp293/VEGFR2 transfected with NRP1 as well as HUVEC and CASMC, both of which are reported to endogenously express NRP1. As shown in Fig. 2A, we could detect co-immunoprecipitated CSNK2A1 with NRP1 not only in NRP1 transfected Flp293/VEGFR2 cells but also in HUVEC and CASMC without forced expression. Intriguingly, co-immunoprecipitated CSNK2A1 was more prominent in HUVEC than in CASMC, despite NRP1 is well expressed in both HUVEC and CASMC [9]. To further

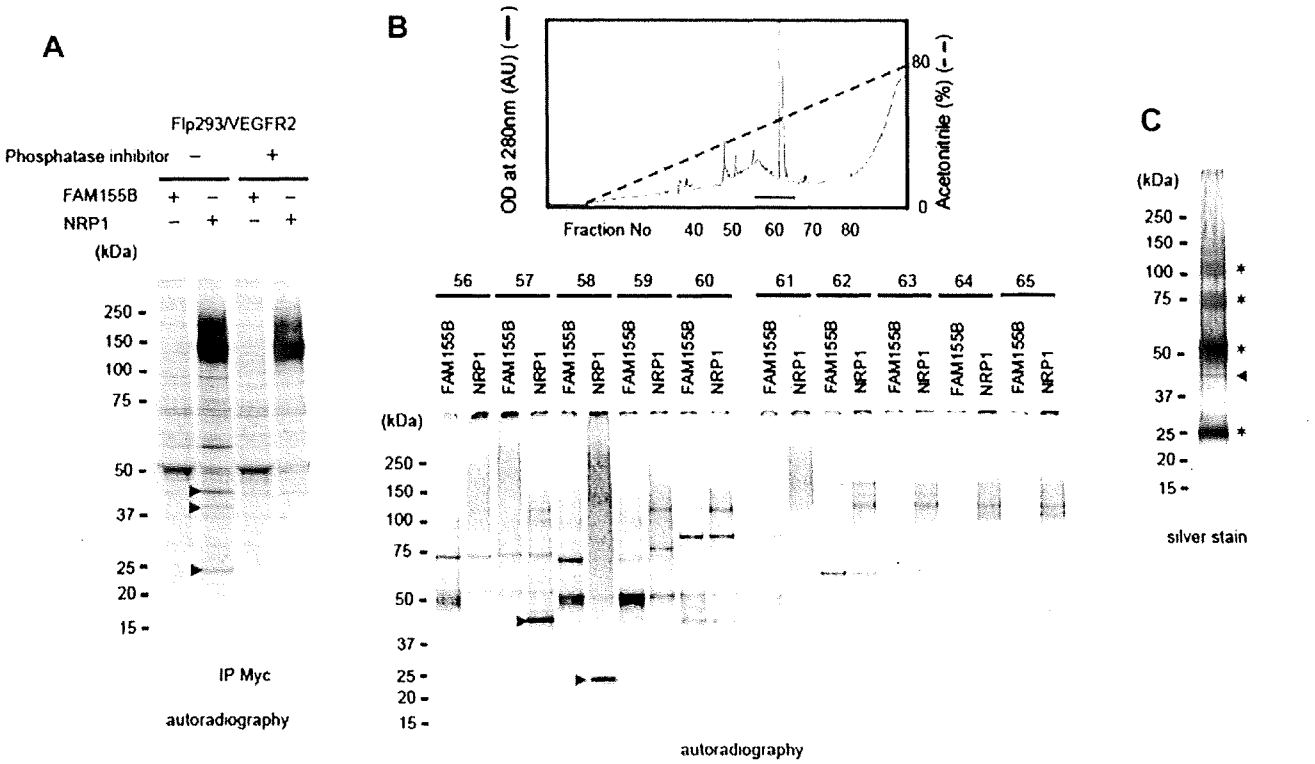

Fig. 1. Identification of protein kinase CK2 as a novel NRP1 binding protein. (A) NRP1 immunoprecipitates using metabolic labelling with ^{35}S in Flp293/VEGFR2 cells showed that 3 candidate bands (arrowheads) were specifically associated with NRP1 (lane 2). Phosphatase inhibitors decreased this interaction (lane 4). Myc-tagged human FAM155B (NM_015686.2) which is unrelated to VEGF signal was used as a control. (B) NRP1-immunoprecipitates were applied to reverse-phase HPLC. The protein was eluted with a linear gradient of 0–80% acetonitrile (Upper panel). Each fraction was separated by SDS–PAGE and visualized by autoradiography (Lower panel). (C) In fraction 57 of large scale preparation without metabolic labelling, the 43 kDa NRP1-associated band (arrowheads) was visualized by silver stain and excised for mass-spectrometry. Asterisks indicated immunoglobulin.

characterize the binding site of NRP1, we constructed several NRP1 deletion mutants (Fig. 2B) which were tested in the co-immunoprecipitation studies. As for intact NRP1, the 43 kDa NRP1-associated band which was revealed to be CSNK2A1 was detected in all constructs except for del B mutant (asterisk in Fig. 2C), suggesting that the interaction between CSNK2A1 and NRP1 occurs at extracellular b1b2 domain of NRP1. It is of note that all three NRP1 associating bands (asterisk and arrowheads in Fig. 2C) disappeared in del B mutant, while they were seen in all other constructs.

Protein kinase CK2 is a holoenzyme which consists of heterotetramer of catalytic subunits (α (CSNK2A1) and α′ (CSNK2A2)) and regulatory β (CSNK2B) subunits conforming $\alpha_2\beta_2$, $\alpha\alpha'\beta_2$ and $\alpha'_2\beta_2$ combinations. As the molecular weights of CSNK2A2 and CSNK2B are 40 and 25 kDa, respectively, we presume 3 NRP1-associated bands (asterisks in Fig. 1A) may correspond to α, α′ and β subunits. Indeed, co-immunoprecipitation using HEK293T cells transfected with FLAG-NRP1 demonstrated that CSNK2B was associated with NRP1 (Fig. 2D).

From these data, we therefore concluded that protein kinase CK2 holoenzyme can bind to NRP1 via its extracellular domain.

NRP1 is phosphorylated by CK2 in vitro and in vivo

As CK2 is reported to be an extracellular kinase [15] and phosphatase inhibitors affected the interaction between CK2 and NRP1 (Fig. 1A), we hypothesized that NRP1 is a substrate for CK2. As shown in Fig. 3A, the purified recombinant NRP1 was strongly phosphorylated by holoenzyme CK2 *in vitro* and this phosphorylation was significantly inhibited by adding the CK2 inhibitor, DMAT. Using purified deletion mutants of NRP1 as a substrate for the *in vitro* kinase assay, phosphorylation of NRP1 by CK2 was completely absent in del B mutant (Fig. 3B), suggesting that CK2 phosphorylates NRP1 at its extracellular b1b2 domain in addition to being the binding site. Phosphoamino acid analysis of digested phosphorylated NRP1 revealed that the phosphorylation of NRP1 by CK2 holoenzyme occurred in both threonine and serine residues, but not tyrosine residue (Fig. 3C).

As phosphorylation of NRP1 has not been reported before, we further checked this phosphorylation of NRP1 *in vivo*. HUVEC transfected with either FLAG-tagged NRP1 adenovirus or LacZ expressing adenovirus, were metabolically labelled with ortho ^{32}P, then subjected to immunoprecipitation by anti-FLAG Ab or anti-NRP1 Ab. As shown in Fig. 3D, the distinct single band which corresponds to NRP1 in molecular weight was clearly labelled by ^{32}P, and that this phosphorylation was not affected by VEGF. In addition, the extent of phosphorylation of NRP1 was decreased by the pre-incubation of cells with DMAT, the CK2 inhibitor (Fig. 3E). These data suggest that NRP1 is phosphorylated by CK2 *in vivo*.

Discussion

In this study, we identified the novel NRP1 binding protein, CK2 holoenzyme in our combined purification strategy using epitope-tag immunoprecipitation followed by reverse-phase HPLC. We also demonstrated that NRP1 is phosphorylated by CK2 both *in vitro* and *in vivo*.

Although NRP1 is considered to work as a co-receptor that binds extracellular ligands and forms receptor complexes with

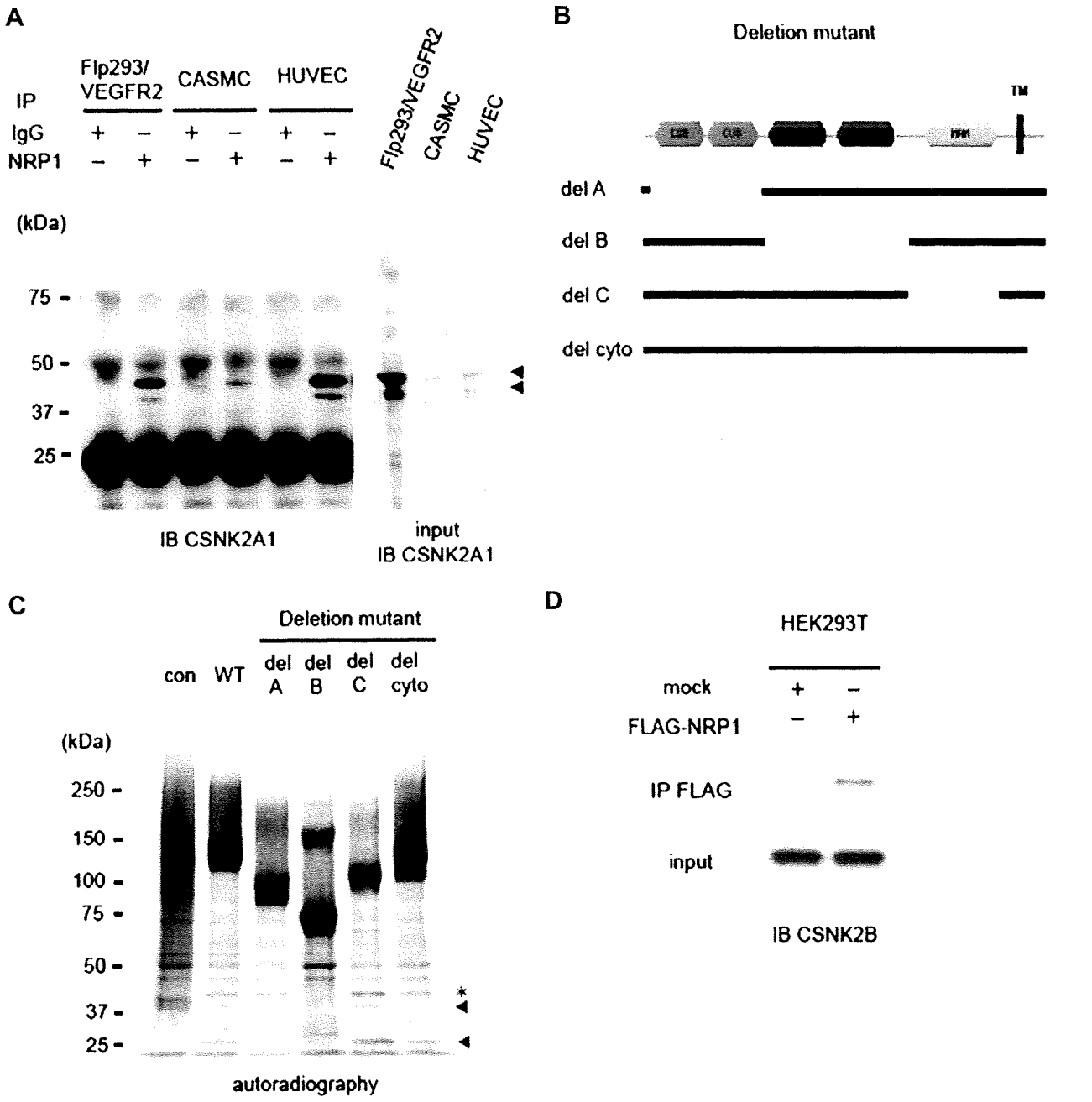

Fig. 2. Protein kinase CK2 binds NRP1 via its extracellular domain. (A) CSNK2A1 (arrowheads) was co-immunoprecipitated with NRP1 in either Flp293/VEGFR2 transfected with NRP1, human umbilical vein endothelial cells (HUVEC) or human coronary artery smooth muscle cells (CASMC). As input, 5% of whole cell lysates were used (right panel). Non-specific IgG was used as an immunoprecipitation control. (B) Schematic model of the NRP1 deletion mutants. CUB; complement protein subcomponents Clr/Cls, Urchin embryonic growth factor and Bone morphogenic protein domain, MAM; Meprin/A5-protein/PTPmu domain, TM; transmembrane. (C) NRP1 immunoprecipitates using metabolic labelling with ^{35}S showed 3 NRP1-associating bands (arrowheads) could be detected in all constructs except for del B mutant. (D) Co-immunoprecipitation using HEK293T cells transfected with FLAG-NRP1 demonstrated that CSNK2B was associated with NRP1.

the signalling receptors involved (VEGFRs or plexins), this model does not fully explain all the lines of evidence relating to the functions of NRP1 in endothelial cells and other cell types [7,16,17]. NRP1 was reported to be able to homodimerize or oligomerize through its binding to heparan sulfate [18]. Further, we and others recently reported that NRP1 is modified by negatively charged-glycosaminoglycan chains [9]. Recently, Sarris et al. demonstrated that NRP1 localises in immunological synapse where multi-signalling molecules can form a complex and initiate an immune response [11]. All this evidence suggests that NRP1 acts like scaffold protein which can form a multi-signalling molecular complex [12]. Therefore, the identification of novel molecular interactions with NRP1 is likely to provide a new aspect to help understand NRP1 functions.

Here we identified CK2 as a novel associating partner of NRP1 and this interaction occurs at the extracellular domain of NRP1. Protein kinase CK2 is present in the cytoplasm, nuclei, and several other organelles. In addition, this enzyme has been recently found bound to the external side of the cell membrane where it acts as an ectokinase phosphorylating several extracellular proteins [19–21].

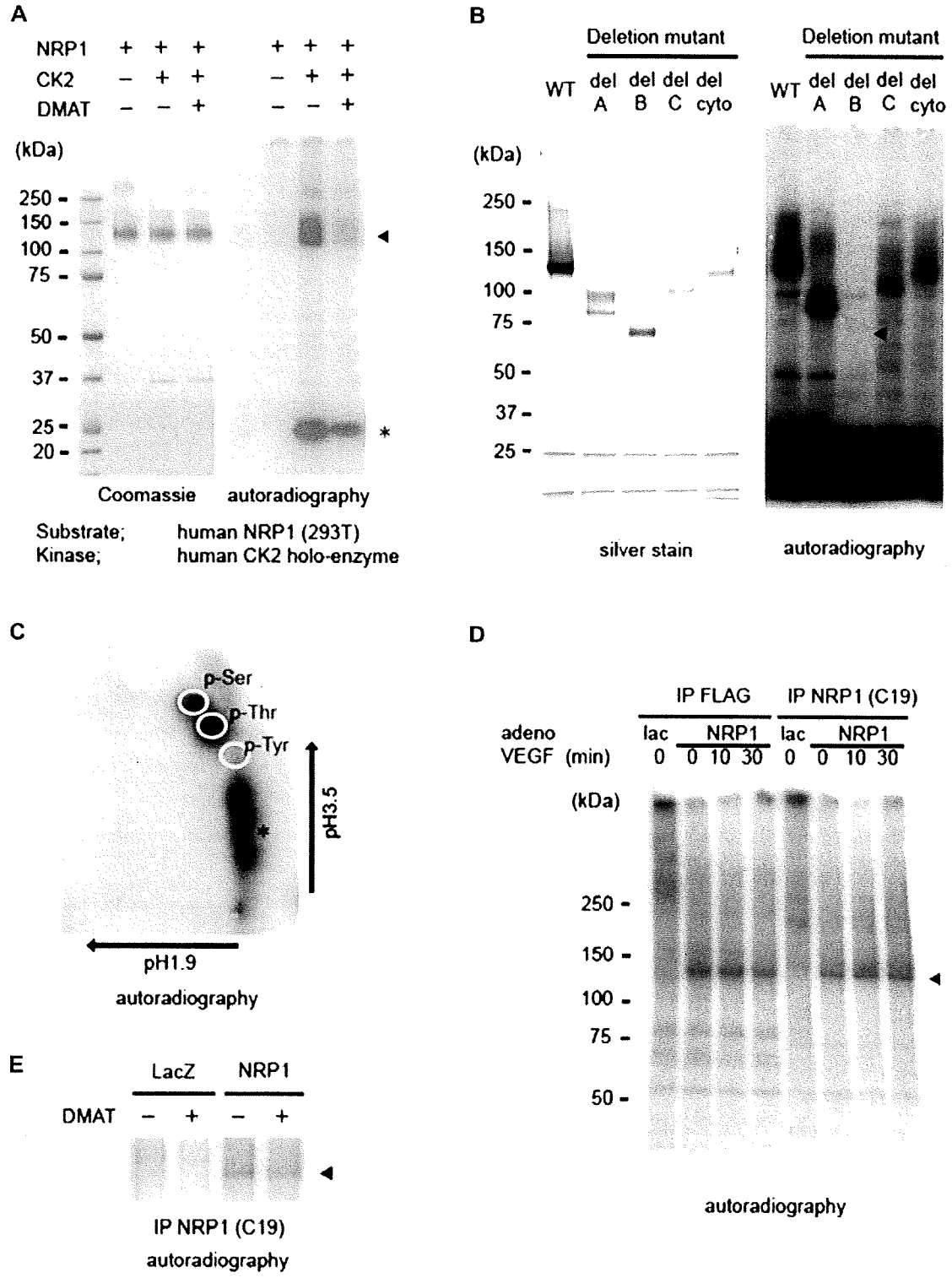

Fig. 3. Protein kinase CK2 phosphorylates NRP1 at its extracellular domain *in vitro* and *in vivo*. (A) FLAG-NRP1 purified from HEK293T was incubated with recombinant CK2 holoenzyme in the presence of [γ-^{32}P] ATP at 30 °C for 60 min, and then the reaction mixture was analyzed by SDS–PAGE, stained with Coomassie blue, and visualized by autoradiography. NRP1 was clearly phosphorylated by CK2, this phosphorylation was significantly blocked by the CK2 inhibitor, DMAT (1 μM). Asterisk shows autophosphorylated CK2β subunit (CSNK2B). (B) Deletion mutants of FLAG-NRP1 purified from HEK293T were used for the *in vitro* kinase assay as described in (A). Phosphorylation of NRP1 by CK2 was completely absent in the del B mutant. Arrowhead shows absent phosphorylation in del B mutant. (C) Phosphoamino acid analysis of phosphorylated NRP1. Phosphorylated NRP1 *in vitro* was excised from the gel, digested with trypsin, and hydrolyzed in hydrochloric acid. The resulting phosphoamino acids were separated by thin-layer electrophoresis using pH 1.9 for the first dimension and pH 3.5 for the second dimension. Autoradiography shows radiolabelled material co-migrating with the phosphoserine (pSer) and phosphothreonine (pThr) standards, but not with phosphotyrosine (pTyr) standard. Asterisk shows incomplete hydrolysis. (D) *In vivo* ^{32}P labelling in HUVEC transfected by either LacZ or FLAG-NRP1 adenovirus demonstrated that NRP1 was phosphorylated *in vivo* (arrowhead). VEGF (50 ng/ml) was added as indicated time course. (E) CK2 inhibitor, DMAT pretreatment (1 μM) decreased NRP1 phosphorylation *in vivo*. The experimental protocol was same as in (D).

Protein kinase CK2 is a holoenzyme which consists of heterotetramer of catalytic and regulatory subunit, and previous reports suggested that expression of both subunits is necessary for the appearance of the ectopic enzyme as an ectokinase [15]. Therefore our findings that NRP1 immunoprecipitates contains 3 bands (which corresponds to catalytic subunits α, α′ and regulatory β subunit) is consistent with the biology of ectokinase CK2.

The identification of an ectokinase with catalytic properties on the cell surface shed new light on the potential role of extracellular phosphorylation on a number of physiological and pathological processes [22]. Protein kinase CK2 is one of the major ectokinases and CK2-mediated extracellular phosphorylation has been reported in regulating cellular functions; cell adhesion [19,20], neurite regeneration [21] and lytic activity [23]. As NRP1 was originally considered as an adhesion molecule [24], and known to interact with L1CAM adhesion molecule [25], the interaction between CK2 and NRP1 or CK2 mediated NRP1 phosphorylation might be involved in regulating cell–cell interactions.

In summary, we identified ectokinase CK2 as a novel binding partner for NRP1, and that this protein kinase phosphorylates NRP1 *in vitro* and *in vivo*. Although future investigation will be needed to clarify the physiological importance of this interaction/phosphorylation of NRP1 by CK2, these data add new insight into the understanding of the biology of NRP1.

Acknowledgments

We thank A. Ogai, Y. Nagamachi and H. Okuda for technical assistance. We also thank Dr. S. Coppen for critical reading of the manuscript. This research was supported by grants-in-aid from the Ministry of Health, Labor, and Welfare-Japan; grants-in-aid from the Ministry of Education, Culture, Sports, Science, and Technology-Japan; grants from the Japan Heart Foundation; grants from the Japan Cardiovascular Research Foundation; a grant from the Japan Society for the Promotion of Science; a grant from the Mochida Memorial Foundation for Medical and Pharmaceutical Research; a grant from Grant-in-Aid of the Japan Medical Association and the National BioResource Project from the Ministry of Education, Culture, Sports, Science, and Technology of Japan. Y.S. is a Research Fellow of the Japan Society for the Promotion of Science.

References

[1] A.L. Kolodkin, D.V. Levengood, E.G. Rowe, Y.T. Tai, R.J. Giger, D.D. Ginty, Neuropilin is a semaphorin III receptor, Cell 90 (1997) 753–762.
[2] S. Soker, S. Takashima, H.Q. Miao, G. Neufeld, M. Klagsbrun, Neuropilin-1 is expressed by endothelial and tumor cells as an isoform-specific receptor for vascular endothelial growth factor, Cell 92 (1998) 735–745.
[3] T. Kitsukawa, M. Shimizu, M. Sanbo, T. Hirata, M. Taniguchi, Y. Bekku, T. Yagi, H. Fujisawa, Neuropilin–semaphorin III/D-mediated chemorepulsive signals play a crucial role in peripheral nerve projection in mice, Neuron 19 (1997) 995–1005.
[4] T. Kawasaki, T. Kitsukawa, Y. Bekku, Y. Matsuda, M. Sanbo, T. Yagi, H. Fujisawa, A requirement for neuropilin-1 in embryonic vessel formation, Development 126 (1999) 4895–4902.
[5] G. Neufeld, O. Kessler, The semaphorins: versatile regulators of tumour progression and tumour angiogenesis, Nat. Rev. Cancer 8 (2008) 632–645.
[6] A. Bagri, M. Tessier-Lavigne, R.J. Watts, Neuropilins in tumor biology, Clin. Cancer Res. 15 (2009) 1860–1864.
[7] R. Tordjman, Y. Lepelletier, V. Lemarchandel, M. Cambot, P. Gaulard, O. Hermine, P.H. Romeo, A neuronal receptor, neuropilin-1, is essential for the initiation of the primary immune response, Nat. Immunol. 3 (2002) 477–482.
[8] D. Ghez, Y. Lepelletier, S. Lambert, J.M. Fourneau, V. Blot, S. Janvier, B. Arnulf, P.M. van Endert, N. Heveker, C. Pique, O. Hermine, Neuropilin-1 is involved in human T-cell lymphotropic virus type 1 entry, J. Virol. 80 (2006) 6844–6854.
[9] Y. Shintani, S. Takashima, Y. Asano, H. Kato, Y. Liao, S. Yamazaki, O. Tsukamoto, O. Seguchi, H. Yamamoto, T. Fukushima, K. Sugahara, M. Kitakaze, M. Hori, Glycosaminoglycan modification of neuropilin-1 modulates VEGFR2 signaling, EMBO J. 25 (2006) 3045–3055.
[10] C. Pellet-Many, P. Frankel, H. Jia, I. Zachary, Neuropilins: structure, function and role in disease, Biochem. J. 411 (2008) 211–226.
[11] M. Sarris, K.G. Andersen, F. Randow, L. Mayr, A.G. Betz, Neuropilin-1 expression on regulatory T cells enhances their interactions with dendritic cells during antigen recognition, Immunity 28 (2008) 402–413.
[12] K.A. Uniewicz, D.G. Fernig, Neuropilins: a versatile partner of extracellular molecules that regulate development and disease, Front. Biosci. 13 (2008) 4339–4360.
[13] E. Geretti, A. Shimizu, M. Klagsbrun, Neuropilin structure governs VEGF and semaphorin binding and regulates angiogenesis, Angiogenesis 11 (2008) 31–39.
[14] H. Kato, S. Takashima, Y. Asano, Y. Shintani, S. Yamazaki, O. Seguchi, H. Yamamoto, A. Nakano, S. Higo, A. Ogai, T. Minamino, M. Kitakaze, M. Hori, Identification of p32 as a novel substrate for ATM in heart, Biochem. Biophys. Res. Commun. 366 (2008) 885–891.
[15] F. Rodriguez, C.C. Allende, J.E. Allende, Protein kinase casein kinase 2 holoenzyme produced ectopically in human cells can be exported to the external side of the cellular membrane, Proc. Natl. Acad. Sci. USA 102 (2005) 4718–4723.
[16] P. Frankel, C. Pellet-Many, P. Lehtolainen, G.M. D'Abaco, M.L. Tickner, L. Cheng, I.C. Zachary, Chondroitin sulphate-modified neuropilin 1 is expressed in human tumour cells and modulates 3D invasion in the U87MG human glioblastoma cell line through a p130Cas-mediated pathway, EMBO Rep. 9 (2008) 983–989.
[17] Q. Pan, Y. Chanthery, W.C. Liang, S. Stawicki, J. Mak, N. Rathore, R.K. Tong, J. Kowalski, S.F. Yee, G. Pacheco, S. Ross, Z. Cheng, J. Le Couter, G. Plowman, F. Peale, A.W. Koch, Y. Wu, A. Bagri, M. Tessier-Lavigne, R.J. Watts, Blocking neuropilin-1 function has an additive effect with anti-VEGF to inhibit tumor growth, Cancer Cell 11 (2007) 53–67.
[18] C.W. Vander Kooi, M.A. Jusino, B. Perman, D.B. Neau, H.D. Bellamy, D.J. Leahy, Structural basis for ligand and heparin binding to neuropilin B domains, Proc. Natl. Acad. Sci. USA 104 (2007) 6152–6157.
[19] V. Stepanova, U. Jerke, V. Sagach, C. Lindschau, R. Dietz, H. Haller, I. Dumler, Urokinase-dependent human vascular smooth muscle cell adhesion requires selective vitronectin phosphorylation by ectoprotein kinase CK2, J. Biol. Chem. 277 (2002) 10265–10672.
[20] H.T. Nguyen, G. Dalmasso, Y. Yan, T.S. Obertone, S.V. Sitaraman, D. Merlin, Ecto-phosphorylation of CD98 regulates cell–cell interactions, PLoS ONE 3 (2008) e3895.
[21] Y. Takei, Phosphorylation of Nogo receptors suppresses Nogo signaling, allowing neurite regeneration, Sci. Signal. 2 (2009) ra14.
[22] D. Kubler, W. Pyerin, E. Burow, V. Kinzel, Substrate-effected release of surface-located protein kinase from intact cells, Proc. Natl. Acad. Sci. USA 80 (1983) 4021–4025.
[23] O. Bohana-Kashtan, L.A. Pinna, Z. Fishelson, Extracellular phosphorylation of C9 by protein kinase CK2 regulates complement-mediated lysis, Eur. J. Immunol. 35 (2005) 1939–1948.
[24] S. Takagi, Y. Kasuya, M. Shimizu, T. Matsuura, M. Tsuboi, A. Kawakami, H. Fujisawa, Expression of a cell adhesion molecule, neuropilin, in the developing chick nervous system, Dev. Biol. 170 (1995) 207–222.
[25] V. Castellani, E. De Angelis, S. Kenwrick, G. Rougon, Cis and trans interactions of L1 with neuropilin-1 control axonal responses to semaphorin 3A, EMBO J. 21 (2002) 6348–6357.

Journal of Molecular and Cellular Cardiology xxx (2009) xxx–xxx

Contents lists available at ScienceDirect

Journal of Molecular and Cellular Cardiology

journal homepage: www.elsevier.com/locate/yjmcc

Review article

ER stress in cardiovascular disease

Tetsuo Minamino [a,*], Masafumi Kitakaze [b]

[a] Department of Cardiovascular Medicine, Osaka University Graduate School of Medicine, 2-2 Yamadaoka, Suita 565-0871, Osaka, Japan
[b] Department of Cardiovascular Medicine, National Cardiovascular Center, Suita 565-8565, Osaka, Japan

ARTICLE INFO

Article history:
Received 1 September 2009
Accepted 28 October 2009
Available online xxxx

Keywords:
Endoplasmic reticulum
ER stress
Heart failure
Anti-cancer drug
Atherosclerosis
Plaque rupture

ABSTRACT

The endoplasmic reticulum (ER) is an organelle involved in protein folding, calcium homeostasis, and lipid biosynthesis. Various factors that interfere with ER function lead to accumulation of unfolded proteins, including oxidative stress, ischemia, disturbance of calcium homeostasis, and overexpression of normal and/or incorrectly folded proteins. The resulting ER stress triggers the unfolded protein response (UPR) that induces signal transduction events to reduce the accumulation of unfolded proteins by increasing ER resident chaperones, inhibiting protein translation, and accelerating the degradation of unfolded proteins. However, if stress is severe and/or prolonged, the ER also initiates apoptotic signaling that includes induction of the pro-apoptotic transcriptional factor C/EBP homologous protein, activation of c-Jun amino-terminal kinase, and cleavage of caspase-12. These ER-initiated events lead to cell death via mitochondria-dependent and -independent apoptotic pathways. Furthermore, the B cell lymphoma 2 family of proteins expressed on the ER and mitochondria are also involved in regulating cell death due to ER stress. Thus, the ER is now recognized as a vitally important organelle that can decide cell survival or death. Recent animal and human studies have revealed that the UPR and ER-initiated apoptosis are implicated in the pathophysiology of various cardiovascular diseases, including heart failure, ischemic heart disease, the development of atherosclerosis, and plaque rupture. Improved understanding of the molecular mechanisms underlying UPR activation and ER-initiated apoptosis in cardiovascular disease will provide us with new targets for drug discovery and therapeutic intervention.

Contents

1. Introduction

The endoplasmic reticulum (ER) is an organelle that has an essential role in multiple cellular processes, such as the folding of secretory and membrane proteins, calcium homeostasis, and lipid biosynthesis [1,2]. A variety of insults can interfere with ER function, leading to the accumulation of unfolded and misfolded proteins in the ER. When ER transmembrane sensors detect the accumulation of unfolded proteins, the unfolded protein response (UPR) is initiated to cope with the resulting ER stress. If ER stress is prolonged or overwhelming, however, it can induce cell death. Recent studies have suggested that the UPR and ER-initiated apoptosis are implicated in the pathophysiology of various human

* Corresponding author. Tel.: +81 6 6879 3635; fax: +81 6 6879 3473.
E-mail address: minamino@cardiology.med.osaka-u.ac.jp (T. Minamino).

0022-2828/$ – see front matter © 2009 Elsevier Inc. All rights reserved.
doi:10.1016/j.yjmcc.2009.10.026

diseases, including cardiovascular disease, neurodegenerative disease, diabetes mellitus, and liver disease [1-3]. This review summarizes (1) the molecular mechanisms of the UPR and ER-initiated apoptosis and (2) their involvement in the pathophysiology of cardiovascular disease.

2. The endoplasmic reticulum

The ER is recognized as the organelle involved in the synthesis and folding of secreted and membrane-bound proteins and thus is the first part of the secretory pathway [1-3]. The ER supports the biosynthesis of approximately one third of all cellular proteins in a typical eukaryotic cell [4]. To achieve the proper folding of proteins, the lumen of the ER is a special environment [1,2], e.g., the ER has the highest calcium concentration within the cell. Both protein folding reactions and the functioning of various calcium-dependent ER resident chaperones require a high level of calcium. Furthermore, an oxidizing environment inside the ER is crucial for the formation of disulfide bonds that is required for the proper folding of proteins. As a consequence of these special requirements, ER function is highly sensitive to stresses that disturb calcium homeostasis or alter the intraluminal redox status.

3. UPR signaling

When ER stress occurs, three ER transmembrane sensors are activated to initiate adaptive responses [1-3]. These sensors include protein kinase-like ER kinase (PERK), inositol-requiring kinase 1 (IRE1), and the transcriptional factor activating transcription factor 6 (ATF6). These UPR sensors are located with their N-terminus inside the lumen of the ER and their C-terminus in the cytosol, thereby connecting the ER with the cytosol. All three sensors are maintained in an inactive state through the interaction of their N-terminus with glucose-regulated protein 78 kDa (GRP78) [5]. When unfolded proteins accumulate in the ER, GRP78 releases these sensors to allow their oligomerization and thereby initiates the UPR [5] (Fig. 1).

PERK is a serine threonine kinase that phosphorylates eukaryotic translation initiation factor 2α (eIF2α) after the onset of ER stress to shut off mRNA translation and reduce the protein load on the ER. Paradoxically, however, several mRNAs require the phosphorylation of eIF2α for their translation, including the transcriptional factor ATF4 that induces UPR-related genes to reduce the level of unfolded proteins in the ER.

IRE1α is the most fundamental ER stress sensor and is conserved in all eukaryotic cells. Interestingly, activation of IRE1 elicits endoribonelease activity that specifically cleaves the mRNA encoding the transcriptional factor X-box binding protein 1 (XBP1). This unconventional splicing reaction is required for the translation of transcriptionally active XBP1. Active (spliced) XBP1 binds to ER stress response elements I and II (ERSE-I: CCAAT(N9)CCACG; ERSE-II: ATTGG(N1) CCACG) and to the mammalian UPR element (mUPRE: TGACGTGG/A) to regulate a variety of UPR-related genes [6]. Recent studies showed that XBP1 controls diverse cell type- and condition-specific transcriptional regulatory networks, although it has not been well identified how XBP1 regulates genes in cardiomyocytes [7].

ATF6 is a basic ZIP family transcriptional factor that binds to ERSEs in the promoter region of UPR-related genes. ER stress induces the release of GRP78 from ATF6 and thus permits the translocation of ATF6 from the ER to the Golgi apparatus, where S1P- and S2P-mediated proteolytic cleavage produces a transcriptionally active cytosolic fragment. ATF6 activates a subset of UPR-related genes, including XBP1. The three arms of the UPR (including ATF4, XBP1, and ATF6) coordinately regulate the transcription of various genes encoding ER chaperones and protein folding enzymes in order to reduce the accumulation of unfolded proteins.

4. ER-associated degradation

Another mechanism that reduces the level of misfolded and unfolded proteins in the ER is degradation via the ER-associated protein degradation (ERAD) pathway [1,2]. Most ERAD substrates are ubiquitinated before undergoing degradation by proteasomes. The ERAD mediates retro-translocation of unfolded proteins into the cytosol where these proteins are degraded by the ubiquitin-proteasome machinery.

5. ER-initiated apoptotic signaling

When the UPR fails to control the level of unfolded and misfolded proteins in the ER, ER-initiated apoptotic signaling is induced. Interestingly, all of the ER sensor proteins are responsible for apoptotic signaling as well as for the UPR, but it remains unclear how the cell makes a decision between survival and death (Fig. 2).

IRE1α-dependent apoptotic signaling occurs via diverse pathways. IRE1α interacts with the adaptor protein TNF receptor-associated factor (TRAF) 2. IRE1α and TRAF2 then interact with a mitogen-activated protein kinase kinase kinase, ASK1, which subsequently phosphorylates JNK [8,9].

C/EBP homologous protein (CHOP) is the one of most thoroughly investigated molecules among those involved in ER-initiated apoptotic signaling. CHOP is a pro-apoptotic bZIP transcriptional factor that is mainly regulated by ATF4- and ATF6-dependent pathways [1,2].

Table 1
ER stress and cardiovascular disease.

Diseases	Role of ER stress	Target protein	Refs.
Hypeterophic heart	• Pressure-overload to heart induces UPR	• GRP78	[22]
Failing heart	• ER stress is induced in human failing hearts	• GRP78	[22,23]
	• Pressure-overload to heart finally leads to cardiac apoptosis associated with CHOP induction	• CHOP	[22]
	• Impairment of a retrieval receptor for ER chaperones causes heart failure and CHOP induction	• KDEL/CHOP	[24]
Autoimmune cardiomyopathy	• Autoimmune cardiomyopathy induced by beta-adrenergic receptor peptide is associated with ER stress	• p38/CaMKII • ATF6/GRP78/CHOP	[25]
Alcoholic cardiomyopathy	• Alcohol induces myocardial ER stress	• GRP78/CHOP	[26]
Ischemic heart	• PDI is induced in cardiomyocytes near myocardial infarction in humans	• PDI	[45]
	• GRP94 plays cardioprotective role against hypoxic insult	• GRP94	[46]
	• ATF6 protects the myocardium from ischemic/reperfused myocardium	• ATF6/GRP78/GRP94	[47]
	• Hypoxia induces CHOP and caspase 12 activation, which is inhibited by AMP-activated kinase	• ATF6/GRP78/GRP94	[51]
	• PUMA inhibits cardiomyocyte cell death by ER stress	• PUMA	[52,53]
Cardiotoxicity of anti-cancer drug	• Imatinib induces cardiomyocyte cell death associated with ER stress and JNK activation	• JNK	[31]
	• Proteasome inhibition induces cardiomyocyte cell death via CHOP	• CHOP	[35]
Atherosclerosis	• Oxidative stress causes macrophage apoptosis via CHOP	• CHOP	[39]
	• UPR and ER-initiated apoptosis in macrophage in atherosclerotic lesions		[39,40]
	• Increased CHOP induction in ruptured atherosclerotic plaques	• CHOP	[39,43]

Please cite this article as: Minamino T, Kitakaze M, ER stress in cardiovascular disease, J Mol Cell Cardiol (2009), doi:10.1016/j.yjmcc.2009.10.026